HHS Public Access

Author manuscript

ACS Appl Mater Interfaces. Author manuscript; available in PMC 2016 February 01.

Published in final edited form as:

ACS Appl Mater Interfaces. 2015 March 4; 7(8): 5017–5028. doi:10.1021/acsami.5b00655.

Nanoparticle-Mediated Intracellular Delivery Enables Cryopreservation of Human Adipose-Derived Stem Cells Using Trehalose as the Sole Cryoprotectant

Wei Rao[1,2], **Haishui Huang**[1,2,3], **Hai Wang**[1,2,4], **Shuting Zhao**[1,2], **Jenna Dumbleton**[1,2], **Gang Zhao**[5], and **Xiaoming He**[1,2,4,*]

[1]Department of Biomedical Engineering, The Ohio State University, Columbus, OH 43210, US

[2]Davis Heart and Lung Research Institute, The Ohio State University, Columbus, OH 43210, USA

[3]Department of Mechanical Engineering, The Ohio State University, Columbus, OH 43210, US

[4]Comprehensive Cancer Center, The Ohio State University, Columbus, OH 43210, USA

[5]Centre for Biomedical Engineering, Department of Electronic Science and Technology, University of Science and Technology of China, Hefei, Anhui 230027, China

Abstract

In this study, pH responsive genipin-crosslinked Pluronic F127-chitosan nanoparticles (GNPs) was synthesized to encapsulate trehalose for intracellular delivery to cryopreserve primary human adipose-derived stem cells (hADSCs). Trehalose is a disaccharide of glucose used by lower-organisms to survive extreme cold in nature and has been used to cryopreserve various biomacromolecules. However, it does not enter mammalian cells due to its highly hydrophilic nature and has only been used in combination with other cell-penetrating cryoprotectants such as DMSO to cryopreserve mammalian cells. Our data show that trehalose can be efficiently encapsulated in our GNPs for intracellular delivery, which enables cryopreservation of primary hADSCs using the nontoxic sugar as the sole cryoprotectant. This capability is important because the conventional approach of cryopreserving mammalian cells using highly toxic (at body temperature) cell-penetrating cryoprotectants requires multi-step washing of the cryopreserved cells to remove the toxic cryoprotectant for further use, which is time-consuming and associated with significant cell loss (~10% during each washing step). By contrast, the trehalose-cryopreserved cells can be used without washing, which should significantly facilitate the wide application of the burgeoning cell-based medicine.

*Corresponding Author: Phone: 1 (614) 247-8759. Fax: 1 (614) 292-7301. he.429@osu.edu. Department of Biomedical Engineering, The Ohio State University, 1080 Carmack Road, Columbus, OH.

Author Contributions

X.H. conceived the project; X.H. and W.R. designed the experiments; W.R. performed all the experiments with help from H.H., H.W., and S.Z.; all authors analyzed and discussed the data; X.H. and W.R. wrote the manuscript with contributions from all authors; and all authors reviewed and approved the manuscript.

Supporting Information Available: Tables S1–S2 for data on encapsulation efficiency and loading content and Table S3 for genes and primers used for real time PCR studies. This material is available free of charge via the Internet at http://pubs.acs.org.

Keywords

trehalose; cryopreservation; genipin; nanoparticle; stem cells

INTRODUCTION

With the recent advancements in cell-based medicine, the living cells are becoming increasingly important for healthcare[1–3]. Therefore, it is important to ensure the ready availability of living cells for the burgeoning cell-based medicine. This can be achieved by cell preservation to bank living cells in a state of suspended animation with negligible metabolic and degradative activities[2–9], which is particularly important for stem cells because of the high cost of culturing stem cells at 37 °C and their tendency of spontaneous differentiation and/or possible genetic alterations during continuous long-term culture *in vitro*[10–17]. This suspended state of animation can be achieved by cooling cells to bank in liquid nitrogen, a technology commonly known as cell cryopreservation[2–9]. However, current practice of cell cryopreservation relies on the use of cell membrane-permeable cryoprotectants (usually dimethyl sulfoxide known as DMSO in no less than ~10% in volume) to protect cells from being killed during cooling/freezing/warming between room and cryogenic temperatures[2–9, 18, 19]. Although it is less so below room temperature, the commonly used cryoprotectants are highly toxic at 37 °C (body temperature) and can't be applied to patients. For example, incomplete removal of DMSO from cells has been shown to cause intravascular hemolysis and increased serum transaminase levels in clinic application[20, 21]. In addition, DMSO has been found to induce differentiation of more than 25 human stem cell lines[22]. Therefore, tedious multi-step washing is required to completely remove the highly toxic, cell membrane-permeable cryoprotectants from cryopreserved cells for clinical use, which is often associated with significant loss of the precious cells (~10% during each washing step). Therefore, it is important to achieve cell cryopreservation with nontoxic cryoprotectants.

Trehalose, a non-reducing sugar (disaccharide of glucose, 342 Da), is commonly found in organisms capable of withstanding extreme drought and cold in nature (e.g., water bear and yeast)[23–25]. This is attributed to its exceptional capability of 1) acting as water to form hydrogen bonds with and/or promoting preferential hydration of biomacromolecules so that their functional conformations can be retained during cell dehydration (e.g., by freeze-concentration during cryopreservation)[7, 26–33], and 2) forming a stable glassy matrix with extremely low molecular mobility to suspend any degradative and metabolic activities in the dehydrated state[7, 33–36]. As a result, trehalose has been explored as a nontoxic cryo and lyoprotectant to protect various biologicals including lipids, proteins, nuclear materials, virus, bacteria, platelets, and red blood cells from freezing and drying induced injury[36–42]. For preserving eukaryotic mammalian cells, trehalose must be present both outside and inside them to provide sufficient protection[43, 44]. Unfortunately, mammalian cells generally lack the mechanism to synthesize trehalose endogenously and their plasma membrane is impermeable to the sugar[4, 40, 45]. Therefore, effective intracellular delivery of trehalose is of crucial importance to achieve cryopreservation of eukaryotic mammalian cells using the sugar as the sole cryoprotectant.

Over the past decades, a number of approaches have been explored to introduce trehalose into eukaryotic mammalian cells. The most direct approach is to microinject exogenous trehalose into the cytoplasm of mammalian cells one by one. This approach has been applied successfully to deliver trehalose into mammalian oocytes that are large in size (~100 μm in diameter) and small in quantity (tens or at most hundreds)[44, 46–48]. The trehalose-laden oocytes were found to survive well after cryopreservation. However, this approach is difficult to apply for most eukaryotic mammalian cells that are much smaller (< ~20 μm in diameter) than oocytes and present in large quantities (usually millions to billions). Small eukaryotic mammalian cells have been genetically engineered to synthesize trehalose. This approach requires the constant production of adenoviral vectors that exhibit significant cytotoxicity, particularly at high multiplicities of infection[49–51]. Trehalose has also been introduced into small eukaryotic mammalian cells through engineered or native transmembrane pores[43, 52–54], electroporation[55, 56], fluid phase endocytosis[57–59], and lipid phase transition[59, 60]. Recently, liposomes (~400 nm in diameter) have been investigated as a potential vesicle for intracellular delivery of the sugar[61–63]. Moreover, polymeric nanoparticles made of Pluronic F127 and poly (ethylene imine) have been used to successfully deliver trehalose into mammalian cells[64].

However, a consistent report on cryopreservation of small eukaryotic mammalian cells using trehalose as the sole cryoprotectant is still missing[45, 61, 65]. This could be due to the inability to deliver a sufficient amount of trehalose into the eukaryotic cells using some of the approaches (e.g., fluid phase endocytosis). In addition, cells could be too severely compromised during the delivery step to withstand further freezing or drying induced stresses, considering the highly invasive nature of some of the approaches (e.g., mounting transmembrane pores and electroporation). Therefore, further investigations to develop an effective approach for intracellular delivery of trehalose as the sole cryoprotectant for cell cryopreservation are needed.

Building upon our recent work on synthetizing thermally responsive nanoparticles of Pluronic F127 and chitosan with a core-shell structure[66, 67], we developed a procedure using the Pluronic F127-chitosan nanoparticles (NPs) with further genipin crosslinking to achieve efficient encapsulation of trehalose for effective delivery into primary human adipose derived stem cells (hADSCs) in this study. Moreover, we achieved cryopreservation of the primary hADSCs using trehalose as the sole cryoprotectant with high survival and intact function evaluated by their expression of stem cell genes and proteins and capability of adipogenic, osteogenic, and chondrogenic differentiation post cryopreservation.

2. MATERIALS AND METHODS

2.1 Materials

Pluronic F127 (12.6 kDa, polydispersity index: ~1.4) was obtained from BASF Corp (Wyandotte, MI, USA). Chitosan oligosaccharide of pharmaceutical grade (1.2 kDa, 95% deacetylation) was purchased from Zhejiang golden-shell biochemical Co. Ltd (Zhejiang, China). Genipin and α, α-trehalose dehydrate were purchased from Sigma (St. Louis, MO, USA). The CCK-8 cell proliferation reagent was purchased from Dojindo Molecular Technologies (Rockville, MD, USA). Fetal bovine serum (FBS), penicillin, and

streptomycin were purchased from Invitrogen (Carlsbad, CA, USA). The primary hADSCs and their culture and differentiation media were purchased from Lonza (Allendale, NJ, USA). All other chemicals were purchased from Sigma unless specifically mentioned otherwise.

2.2 Synthesis of Genipin-Crosslinked Pluronic F127-Chitosan Nanoparticles (GNPs) and Encapsulation of Trehalose in GNPs to Obtain Nanoparticle-Encapsulated Trehalose (nTre)

To encapsulate trehalose in GNPs, Pluronic F127-Chitosan nanoparticles (NPs) were synthesized using a procedure detailed elsewhere[67]. In brief, a total of 500 μl of the 4-nitrophenyl chloroformate (4-NPC) activated polymer (300 mg/ml) in dichloromethane was added dropwise into 5 ml of chitosan solution (15 mg/ml) in deionized (DI) water at pH 10 under sonication using a Branson 450 digital sonifier (Danbury, CT, USA) at 16% of maximum amplitude for 3 min. Dichloromethane was then removed by rotary evaporation. The resultant solution was dialyzed against DI water with a Spectra/Por dialysis tube (MWCO, 50 kDa) overnight and further dialyzed against DI water for 3 h using 1000 kDa Spectra/Por dialysis tube. Finally, the sample was freeze-dried for 48 h to obtain dry NPs.

To encapsulate trehalose, 1 mg free trehalose (fTre) and the Pluronic F127-chitosan NPs (10 mg) were soaked in 1 ml DI water at 4 °C when the NPs were swollen with high wall-permeability. After 1 h, the sample was lyophilized at −50 °C for 24 h and further dried at 25 °C for 3 h to remove water both inside and outside the NPs. The dried sample was then put in a humidified oven at 37 °C to shrink the NPs and the shrunken sample was dissolved in 0.9 ml of warm (37 °C) 1x PBS and 100 μl of genipin solution (5 mg/ml in 1x PBS) was added. After further keeping at 37 °C for 8 h, the sample was dialyzed against DI water with 20 kDa Spectra/Por dialysis tube for 8 h to remove non-encapsulated fTre and non-reacted genipin and obtain clean solution of nanoparticle-encapsulated trehalose (nTre). The sample was then freeze-dried for 24 h to obtain dry nTre that can be stored at −20 °C for future use. The same procedures were also used to encapsulate propidium iodide (PI), a small fluorescent molecule to obtain nanoparticle-encapsulated PI (nPI). Empty GNPs were made in the same way except soaking with trehalose or PI.

2.3 Characterization of GNPs and nTre

The morphology of GNPs was visualized using an FEI (Hillsboro, OR, USA) Tecnai G2 transmission electron microscope (TEM), for which a carbon film-coated copper TEM grid was first glow-discharged with a Denton (Moorestown, NJ, USA) DV-502 vacuum evaporator for ~30 s. A total of 1 μl aqueous solution of the GNPs (4 mg/ml) was then dropped on the grid and air-dried for ~6–7 minutes. Afterward, the grid was put in contact with a drop of 12.5 μl 1% (w/v) uranyl acetate solution on a Ted Pella (Redding, CA, USA) PELCO® grid holder pad. Excess solution on the grid was removed by dab drying. All procedures were performed at room temperature.

The size and surface zeta potential of GNPs/nTre were assessed using a Brookhaven (Holtsville, NY, USA) 90 Plus/BI-MAS dynamic light scattering (DLS) instrument by dispersing the nanomaterials at 1 mg/ml in DI water and 1 mM aqueous solution of potassium chloride, respectively, according to the manufacturer’s instructions. The resultant

solutions were then filtered through a 0.45 μm filter and the DLS data were obtained after equilibrating the samples at the desired temperatures for at least 30 min.

For characterization using ^{1}H nuclear magnetic resonance (NMR), materials were dissolved in deuterated water (D_2O) and ^{1}H NMR spectra were obtained using a Bruker (Billerica, MA, USA) DPX 400 MHz NMR with D_2O as the internal reference. For Fourier transform infrared spectroscopy (FTIR) study, 5 mg of materials were mixed with 80 mg potassium bromide powder by grinding. The mixture was then molded into a thin film by pressing it between two stainless steel plates and the film was inserted into the sample holder for obtaining the FTIR spectra using a Thermo Nicolet Nexus 870 FTIR instrument.

2.4 Encapsulation Efficiency (EE) and Loading Content (LC)

To determine EE (the weight percentage of trehalose in nanoparticles out of trehalose/PI initially fed for encapsulation) and LC (the weight percentage of trehalose in nanoparticles out of the total weight of both trehalose and nanoparticles), the amount of trehalose concentration in various samples was determined using a trehalose assay kit (Megazyme, Wicklow, Ireland) by following the manufacturer's instructions. In brief, trehalose in a sample was phosphorylated using hexokinase and adenosine-5'-triphosphate (ATP) into glucose-6-phosphate (G-6-P). In the presence of glucose-6-phosphate dehydrogenase (G6P-DH), the produced G-6-P was oxidized by nicotinamide-adenine dinucleotide phosphate ($NADP^+$) into gluconate-6-phosphate and reduced nicotinamide-adenine dinucleotide phosphate (NADPH). The absorbance at 340 nm of NADPH was then measured using a Beckman Coulter DU800 UV-Vis spectrophotometer to determine the amount of trehalose in the sample. The amount of PI was quantified colorimetrically by dispersing nPI in DI water and measure the absorbance at 494 nm with a Beckman Coulter DU800 UV-Vis spectrophotometer (Indianapolis, IN, USA).

2.5 Cell Culture

Primary human adipose-derived stem cells (hADSCs) (Lonza) were cultured in hADSC basal medium (Lonza) supplemented with 10% fetal bovine serum (FBS), 5 ml L-glutamine (Lonza) and 0.5 ml gentamicin-amphotericin (Lonza) at 37 °C in humidified atmosphere with 5% CO_2. Medium was changed every other day. Cells at ~80% confluence were detached for passaging and/or further experimental use. Only cells at or before passage 5 were used.

2.6 Cytotoxicity of GNPs

To check the potential cytotoxicity of GNPs, hADSCs were seeded in 48-well plates at a density of 15,000 cells per well in 250 μl medium. After overnight culture, the cells were treated with empty GNPs at various concentrations (0.1–10 mg/ml). Fresh cells without any treatment (i.e., 0 mg/ml GNPs) were studied in parallel. After culturing for 3 days, the medium containing GNPs was removed and the cells washed using 1x PBS twice. A total of 250 μl of fresh medium and 25 μl of CCK-8 reagent were then added into each well. After incubating for 4 h at 37 °C, absorbance at 450 nm was measured using a Perkin Elmer (Waltham, MA, USA) VICTOR^{TM} X4 Multilabel plate reader to quantify cell number in each well according to a standard line made with the known number of cells in each well

according to the manufacturer's instructions. Cell proliferation was further calculated as the ratio of the cell number determined for each sample to that of fresh cells with no GNP treatment on day 1.

2.7 Cell Uptake

To visualize cell uptake of nPI with Zeiss (Oberkochen, Germany) ApoTome (confocal-like[68]) structured illumination microscopy (SIM), type I collagen-coated glass coverslips (12 mm) were placed in 35 mm Petri dish and hADSCs were seeded in the dish at 1×10^5 cells/dish in 1 ml medium for attaching on the coverslips during overnight incubation. The collagen-coated glass coverslips were made by dipping the glass coverslips in type I collagen solution (1 mg/ml) in 1x PBS for 1 min and drying for 15 min in air at room temperature[69]. The cells were then treated with medium containing nPI (0.08 mM) for up to 24 h at 37 °C. Afterward, the cells were washed twice with 1x PBS and fixed with 4% paraformaldehyde at 37 °C for 10 min. The fixed cells were further incubated with SYTO® 16 green (5 μM in 1x PBS) for 10 min at 37 °C to stain the cell nuclei. After washing twice with 1x PBS at 37 °C, the coverslip with attached cells was mounted onto a glass slide with mounting medium for examination using a Zeiss Axiovert Observer.Z1 microscope with ApoTome SIM capability. Control cells treated with fPI or a simple mixture of fPI and GNPs were studied in the same way in parallel.

To quantify cell uptake of nPI using flow cytometry, hADSCs were seeded in 6-well plate at a density of 1×10^5 cells/well in 1 ml medium and cultured overnight. The cells were then incubated with medium containing nPI (0.08 mM). At the desired times (1, 6, and 24 h), the cells were washed twice with 37 °C 1x PBS, detached using trypsin/ethylenediaminetetraacetic acid (EDTA), washed again with 1x PBS at 37 °C, and analyzed using a BD (Franklin Lakes, NJ, USA) LSR-II Flow Cytometer (excited at 488 nm and detected through 530/30 nm band pass filter) and Diva software.

2.8 Cryopreservation of hADSCs

To cryopreserve hADSCs, the cells were seeded in 6-well plate at a density of 1×10^5 cells/well in 1 ml medium. After overnight incubation, the cells were further incubated in medium with GNPs, fTre, or nTre for 24 h. Cells incubated in medium without any further supplement (i.e., no pre-treatment or NPT) were also prepared in the same way for control. The cells were then washed with 1x PBS, detached using trypsin/EDTA, and collected by centrifugation at 188 g for 5 min. The collected cells were then washed with 1x PBS and re-suspended in 200 μl hADSC culture medium containing 200 mM free trehalose. The cell suspension was transferred into a 1 ml cryovial (Fisher scientific, Pittsburgh, PA, USA) and the cryovial was hermetically sealed before putting in a Thermo Nalgene freezing container that cools/freezes the sample at approximately -1 °C/min to −80 °C in a −80 °C freezer. On the second day, the cryovials were transferred into liquid nitrogen tank for storage. For cryopreservation with DMSO, the detached hADSCs were re-suspended in 200 μl cell culture medium with 10% v/v DMSO in 1 ml cryovial and cryopreserved in the same way using the Thermo Nalgene freezing container. After 1 day storage, the cryovials were removed from the liquid nitrogen tank and thawed in 37 °C water bath. The cells were then washed with 10 ml medium for further analysis.

2.9 Cell Viability, Attachment Efficiency, and Proliferation Post Cryopreservation

The immediate cell viability post cryopreservation was evaluated using the standard live/dead assay kit (Invitrogen, Carlsbad, CA, USA) with calcein AM to identify cells with metabolic activity and ethidium homodimer to check the cell membrane integrity. The collected cells post cryopreservation were re-suspended in 1 ml fresh medium including 9 μM calcein AM and 9 μM ethidium homodimer in a Petri dish and incubated for 10 minutes at 37 °C. ApoTome SIM (10 x objective) phase and fluorescence images were then taken to count the immediate cell viability. The total cell number under each field was determined using phase images. Cells that excluded ethidium homodimer (red) and maintained calcein (green) were taken as viable while cells stained with ethidium homodimer (red) were taken as dead. At least ten randomly selected fields were used for each sample. The immediate cell viability was calculated as the ratio of the number of viable cells to the total number of cells per field (10x).

To quantify cell attachment efficiency, 1.5×10^4 fresh or cryopreserved hADSCs were seeded in 48-well plate. After one-day incubation, the medium was removed and the cells washed using 1x PBS twice. A total of 250 μl fresh medium and 25 μl of CCK-8 reagent were then added to each well. After incubating for 4 h at 37 °C, absorbance at 450 nm was measured to quantify cell number in each sample as aforementioned. The attachment efficiency was calculated as the percentage of the cell number in the cryopreserved sample out of that in fresh samples.

To quantify cell proliferation, the cell growth was evaluated over a three-day period. The hADSCs cryopreserved with nTre were first seeded in 6 well plates. After one day of culture, the cells were detached and 1.5×10^4 cells were seeded in 48-well plates. Fresh hADSCs without cryopreservation were seeded in the same way to serve as control. At different times (1, 2, and 3 days), the medium was removed and the cells washed using 1x PBS twice. The cell number in each well at different times was then determined using CCK-8 as aforementioned and proliferation was calculated as the ratio of the cell number on day 2 and 3 to the cell number on day 1.

2.10 Functional Characterization of hADSCs

For functional study, fresh and cryopreserved (with nTre) hADSCs were seeded at 1×10^5 cells per petri dish (35 mm) and further cultured for 3 days. Afterwards, three different functional assays were performed to determine if the hADSCs retained intact stemness post cryopreservation. First, the expression of stem cell genes was quantified by quantitative RT-PCR (qRT-PCR), for which total RNAs in hADSCs were isolated using the RNeasy Mini Kit (Qiagen, Gaithersburg, MD, USA). Reverse transcription was then carried out using a GeneAmp 9700 PCR system to generate cDNAs with the iScriptTM cDNA synthesis kit (Bio-Rad, Hercules, CA, USA) and qRT-PCR studies were performed with the SYBR Green mix (Bio-Rad) using a Bio-Rad CFX96 real time PCR instrument. Relative gene expression was calculated with the ΔΔCt method [70] using the built-in Bio-Rad software. The genes studied and the corresponding primers used are listed in Table S3. Klf4, Nanog, Oct4, and Sox2 are stem cell genes and glyceraldehyde 3-phosphate dehydrogenase (GAPDH) was used as the reference (or housekeeping) gene.

Second, expression of two surface markers ($CD44^+$ and $CD31^-$) was analyzed by flow cytometry, for which hADSCs were detached using trypsin/EDTA, washed with 1x PBS, and stained with CD44-FITC (Invitrogen, Carlsbad, CA, USA) and CD31-FITC (Abcam, Cambridge, MA, USA) antibodies separately according to the manufacturer's instructions. The stained samples were analyzed using a BD LSR-II Flow cytometer together with FlowJo software.

Third, the multi-lineage potential of hADSCs was tested by adipogenic, osteogenic, and chondrogenic differentiation. The differentiation assays were conducted according to the manufacturer's instruction. For adipogenic differentiation, 2×10^5 cells were seeded in 2 ml of the hADSC medium that was changed every 2 days until the cell became confluent. A total of 3 cycles of induction/maintenance was then conducted to stimulate adipogenic differentiation. Each cycle consisted of feeding the hADSCs with supplemented adipogenesis induction medium (Lonza) to culture for 3 days, followed by one-day culture in the supplemented adipogenic maintenance medium (Lonza). After 3 complete cycles of induction/maintenance, the cells were cultured for 7 days in the supplemented adipogenic maintenance medium that was changed every 2 days. On the last day of differentiation, adipogenic maintenance medium was removed and the cells were rinsed with 1x PBS and fixed with 2 ml of 4% paraformaldehyde solution for 30 minutes. The fixed cells were rinsed twice with 1x PBS and stained with 1 ml of Oil red O working solution (Cyagen) with 3:2 dilution using distilled water and filtering with 20–25 μm filter paper for 30 minutes. After staining, the cells were rinsed 3 times with 1x PBS for further microscopic analysis that was done using the Nikon 80i microscope equipped with a QImaging Retiga CCD color camera. For osteogenic differentiation, 3×10^4 cells were seeded in 2 ml medium in 0.1% collagen coated 6-well plate to prevent cells from peeling during differentiation. After allowing the cells to adhere to the culture surface by 24-hour culture in the hADSC culture medium, the medium was replaced with osteogenesis induction medium (Lonza) that was changed every 2 days for 3 weeks. Afterward, the osteogenic differentiation medium was removed and the cells were rinsed with 1x PBS and fixed in 2 ml 4% paraformaldehyde solution for 30 min. The fixed cells were rinsed with 1x PBS twice and stained in 1 ml Alizarin red S working solution (Cyagen) for 3 minutes. The stained cells were rinsed 3 times with 1x PBS for further microscopic analysis. For chondrogenic differentiation, 2.5×10^5 hADSCs were washed twice with 1 ml incomplete chondrogenic medium (Lonza). Afterward, the cells were re-suspended in 0.5 ml of complete chondrogenic induction medium (Lonza) at a concentration of 5×10^5 cells ml^{-1}. The cell suspension was then transferred into 15 ml polypropylene culture tubes and centrifuged at 150x g for 5 min at room temperature to form pellets in the tubes. The caps of the tubes were then loosened to allow gas exchange and cell pellets in the tubes were incubated at 37 °C in a humidified atmosphere with 5% CO2. The medium was changed every 2–3 days for 21 days when the pellets were harvested and fixed with 4% paraformaldehyde. The fixed pellets were then embedded with paraffin and stained with Alcian blue assay (Cyagen) for further microscopic analysis. The percentage of area stained by Oil red O (ORO), Alizarin red S (ARS), and Alcian blue (AB) for adipogenic, osteogenic, and chondrogenic differentiation, respectively, was calculated using Matlab R2012a (MathWorks).

2.11 Statistical Analysis

All data are reported as the mean ± standard deviation from at least three independent runs. The statistical significance in mean values between two groups was determined using Microsoft® Excel based on Student's two-tailed t-test assuming equal variance. A p value of less than 0.05 was taken as statistically significant.

3. RESULTS AND DISCUSSION

3.1 Encapsulation of Trehalose in GNPs and Their Characterization

As illustrated in Scheme 1, to encapsulate trehalose, we soaked the sugar with Pluronic F127-chitosan NPs in deionized (DI) water at 4 °C when the NPs were swollen and highly permeable[66]. After removing water by freeze-drying, the sample was warmed to shrink the NPs at 37 °C and further crosslinked using genipin (through the amine groups of chitosan in the NPs)[71–73] to form the genipin-crosslinked NPs (GNPs) with a stabilized shrunken structure. The samples were then dialyzed against water to obtain clean solution of nanoparticle-encapsulated trehalose (nTre) that can further freeze-dried for future use.

We first characterized empty GNPs synthesized using the same procedure shown in Scheme 1 with no trehalose. Successful crosslinking of chitosan in Pluronic F127-chitosan NPs by genipin was first evidenced by the change in color from light brown of the aqueous solution of Pluronic F127-chitosan NPs into a blue solution of GNPs (Scheme 1, note: trehalose is colorless). The formation of GNPs was further confirmed by ^{1}H NMR showing a resonance peak (i) at δ ~ 6.2 ppm that is characteristic of aromatic protons in genipin (Figure 1a). This peak is absent in the ^{1}H NMR spectrum of Pluronic F127-chitosan NPs[67]. Based on the ^{1}H NMR spectrum, the cross-linked and total content of chitosan in the GNPs was determined to be 1.4 ± 0.2% and 8.3 ± 0.7% in weight out of the total GNPs, respectively, indicating there is non-crosslinked primary amine of chitosan in the GNPs.

The FTIR spectra of genipin (GP), Pluronic F127-chitosan NPs, simple mixture of GP and Pluronic F127-chitosan NPs, and GNPs over 400 ~ 4000 cm^{-1} are shown in Figure 1b. The peak at ~1680 cm^{-1} is due to C-O stretching in genipin. In the spectrum of Pluronic F127-chitosan NPs, a peak located at ~1240 cm^{-1} is due to the twisting vibration of $–CH_2$ in Pluronic F127. As expected, these two characteristic peaks show up in the FTIR spectrum of the simple mixture of genipin and Pluronic F127-chitosan NPs. Moreover, compared that of to the mixture, the peak at ~1680 cm^{-1} disappears (or is weakened) in the spectrum of GNPs, probably due to the crosslinking reaction between genipin and chitosan. In addition, the peak at ~1240 cm^{-1} is strengthened for the GNPs, probably due to the stretching of C-N bond formed as a result of the crosslinking reaction.

The shrunken core-shell morphology of the GNPs (after drying in air) is confirmed by TEM images (Figure 1c). The diameter of GNPs in DI water (pH ~5–6) was further determined by dynamic light scattering (DLS) to be 47.7 ± 2.1 nm (Figure 1d), which is slightly larger than that from the TEM image at 22 °C probably due to swelling as a result of hydration of the hydrophilic outer layer of the GNPs in water. The GNPs have a positively charged surface at 37 °C as indicated by its surface zeta potential of 17.0 ± 1.7 mV (Figure 1e), which is presumably due to the remaining primary amine in chitosan and important to facilitate

cellular uptake of the GNPs. This is because mammalian cells have a negatively charged plasma membrane with high electrostatic affinity to positively charged nanoparticles. In addition, the fluorescence spectrum (Figure 1f) shows that the GNPs have a fluorescence emission peak at 461 nm, due to the reaction between genipin and the primary amine in chitosan via nucleophilic attack to open the dihydropyran rings and form nitrogen-containing heterocyclic rings[71, 72, 74], as illustrated in Scheme 1. This blue fluorescence is useful for tracking the GNPs after cellular uptake in cells.

After confirming successful synthesis of the GNPs, we performed encapsulation of trehalose. In addition, we encapsulated PI, a small (668 Da) hydrophilic fluorescence dye that is excluded by live cells, to visualize the encapsulation of small hydrophilic molecules using the GNPs for cellular uptake. First of all, we found that genipin crosslinking can significantly improve the encapsulation efficacy (EE) and loading content (LC) of PI at a 1:10 (PI:NPs) feeding ratio by ~10 times (Table S1), indicating the importance of genipin crosslinking to stabilize the shrunken structure in achieving high encapsulation efficiency. Therefore, we performed encapsulation of trehalose only with genipin crosslinking and the data on the EE and LC of trehalose together with size of the resultant nTre at 22 and 37 °C at two different pH values (5 and 7) for various feeding ratios are given in Table S2. The relevant data of empty GNPs are also shown in the table. Both the EE and LC are dependent on the feeding ratio. For all the feeding ratios, the size of the resultant nTre is not thermally responsive at pH 7 although it is thermally responsive at pH 5. Moreover, the nTre is pH responsive at either 22 or 37 °C. This thermal irresponsiveness in size of the nTre obtained at 1:10 feeding ratio at pH 7 and its pH responsiveness in size at 37 °C are further illustrated in Scheme 1 and shown in Figure 2a. We further performed release study at 37 °C at pH 5 and 7 for both nPI (i.e., GNP-encapsulated PI) and nTre obtained at 1:10 feeding ratio and the results are shown in Figure 2b. The release of PI and trehalose out of the GNPs was significantly faster at pH 5 than 7, suggesting that the acidic pH in late endosomes and lysosomes of mammalian cells should facilitate the release of trehalose/PI from the GNPs after cellular uptake.

3.2 Cell Uptake of GNPs Encapsulated With Propidium Iodide (PI)

We studied cell uptake of the GNP-encapsulated small molecules using nPI due to the fluorescence property of PI for easy visualization using fluorescence microscopy and quantification using flow cytometry. Figure 3a shows typical fluorescence micrographs of hADSCs after incubating them with non-encapsulated or free PI (fPI), a simple mixture of fPI and GNPs, and nPI (all with 0.08 mM PI) for 24 h. As expected, no clear red fluorescence of PI could be observable in the cells incubated with fPI probably because the small hydrophilic molecules could not permeate the cell plasma membrane to enter the cells. There is weak red fluorescence in the cells incubated with the mixture of fPI and GNPs probably because some fPI diffused into the GNPs and was taken up by the cells together with the GNPs as evidenced by the blue fluorescence of GNPs in the cells. By contrast, strong red fluorescence could be observed in the cells incubated with nPI for 24 h. This red fluorescence was visible in the cells even after only 1 h incubation although it is not as strong as that after 24 h incubation. Interestingly, the red fluorescence of PI does not completely overlap with the blue fluorescence of GNPs in the hADSCs, particularly at 24 h.

This observation suggests that the encapsulated PI was probably released out of the GNPs or the GNPs were partially degraded in the cells. Therefore, we performed further flow cytometry studies to quantify the fluorescence intensity of GNPs and PI in the hADSCs at different times and the data are given in Figure 3b–c. Indeed, the fluorescence intensity of GNPs (Figure 3b) is high at 1 h and decreases significantly with further incubation to 6 and 24 h, probably due to degradation of the GNPs. On the contrary, the intensity of PI in the cells increases monotonically with time during the 24 h incubation. We didn't test cellular uptake beyond 24 h since it desired to cryopreserve the cells within one day after their procurement. Nevertheless, our data show that the empty GNPs at a concentration as high as 10 mg/ml do not affect the proliferation of the hADSCs even after 3-day incubation (Figure 3d), which indicates the superior biocompatibility of the GNPs. All these data suggest the great potential of the GNPs as a vehicle for delivering trehalose into the hADSCs to protect them during cryopreservation.

3.3 Cryopreservation of Primary hADSCs Using Trehalose as the Sole Cryoprotectant

For cryopreservation studies, the hADSCs were pre-incubated with empty GNPs, fTre, and nTre for 24 h based on the uptake data shown in Figure 3 and then cryopreserved in liquid nitrogen for 1 day. Fresh cells without cryopreservation and hADSCs cryopreserved in the same way with no pre-treatment (NPT) were also studied in parallel as controls. Moreover, the hADSCs cryopreserved using DMSO were studied as the benchmark control. First, we evaluated the immediate viability post cryopreservation based on membrane integrity (i.e., live/dead dye stain) and typical fluorescence micrographs showing high immediate cell viability of the nTre-pretreated cells post cryopreservation are shown in Figure 4a. The corresponding quantitative data are shown in Figure 4b. The post-cryopreservation viability for the hADSCs either pretreated with fTre/GNCs or with no pretreatment is all low and not significantly different, which indicates pre-incubation with fTre for 24 h does not help the hADSCs to survive cryopreservation probably because fTre cannot enter the cells during pre-incubation. By contrast, pre-incubation with nTre (made at 1:10 feeding ratio and 1.1 ± 0.1 mM in the medium for pre-incubation) significantly increases the post-cryopreservation cell viability to 88.1 ± 7.5% (data not shown in Figure 4b) and the viability is further improved to 91.2 ± 3.4% using a higher concentration of nTre (6.2 ± 0.2 mM, made with 20:1 feeding ratio) for pre-incubation. These data of post-cryopreservation cell viability is similar to that post-cryopreservation with DMSO (88.2 ± 2.2%), which indicates nTre was successfully delivered into the hADSCs to protect the plasma membrane of the cells during cryopreservation.

We further examined the viability of the hADSCs 1 day after cryopreservation by quantifying the attachment efficiency calculated as the percentage of attached live cells post cryopreservation out of to the number of fresh cells after 1 d culture.

As shown in Figure 4c, only a minimal percentage of GNPs or fTre pre-treated cells were able to attach post cryopreservation, which is not significantly different from that of cryopreserved cells with no pre-treatment (NPT). The post-cryopreservation attachment efficiency was much higher for the cells pre-incubated with nTre (59.2 ± 4.1 and 46.3 ± 3.0% for 6.2 and 1.1 mM nTre in the medium for pre-incubation, respectively). Although

this attachment efficiency is lower than that of the cells cryopreserved with DMSO (75.2 ± 5.8 %), using nTre as the sole cryoprotectant could eliminate the tedious multi-step washing to remove the highly toxic cryoprotectant in DMSO-cryopreserved cells for clinical use. Besides being time-consuming, the multi-step washing is associated with significant loss of cells (~10% loss in each step). Moreover, the attached cells post cryopreservation with nTre proliferated similarly to fresh hADSCs (Figure 4d). The morphology of hADSCs post cryopreservation with nTre is also similar to that of fresh hADSCs with no cryopreservation (Figure 4e). These data indicate the cryopreserved hADSCs survived well 3 days after cryopreservation using trehalose delivered into the cells with our nanoparticles as the sole cryoprotectant.

To ascertain functional survival of the hADSCs post cryopreservation with nTre as the sole cryoprotectant, further studies were conducted to assess the stemness and capability of differentiation into multiple lineages of the cryopreserved hADSCs as compared to fresh hADSCs. As shown in Figure 5a, no significant difference was observed between the cryopreserved and fresh cells in terms of expression of four common stem cell genes including Nanog, Sox2, Klf4, and Oct4. Further flow cytometry analyses indicate no significance in the expression of two typical surface markers ($CD44^+$ and $CD31^-$) on the cryopreserved versus fresh hADSCs (Figure 5b). The data on adipogenic, osteogenic, and chondrogenic differentiation of the cryopreserved versus fresh hADSCs are shown Figure 5c. For adipogenic differentiation, no significance was observed between the two groups of cells in terms of Oil red O (ORO) staining of adipocyte-like cells with lipid-filled droplets. For osteogenic differentiation, both groups of cells maintained similar osteogenic potential based on Alizarin red S (ARS) staining of calcific deposition, a major function of osteoblasts. For chondrogenic differentiation, Alcian blue (AB) staining of sulfated proteoglycan deposits that are indicative of the presence of functional chondrocytes is not significantly different between the fresh and cryopreserved hADSCs using trehalose as the sole cryoprotectant.

4. CONCLUSIONS

In this study, we utilized genipin crosslinking to efficiently encapsulate trehalose in the pH responsive genipin-crosslinked Pluronic-F127 nanoparticles (GNPs), which enables successful cryopreservation of hADSCs with high viability and intact function using trehalose as the sole cryoprotectant. This nanoparticle-mediated delivery of trehalose into mammalian cells has great potential for cryopreserving hADSCs and possibly other types of stem cells to facilitate their ready availability for clinical use by putting them in a sweet (due to trehalose, a sugar) dream in liquid nitrogen without the use of any toxic cryoprotectant, which will have a significant impact on the burgeoning cell-based medicine.

Supplementary Material

Refer to Web version on PubMed Central for supplementary material.

Acknowledgments

This work was partially supported by grants from NSF (CBET-1154965) and NIH (R01EB012108).

References

1. Gearhart J. New Potential for Human Embryonic Stem Cells. Science. 1998; 282:1061–1062. [PubMed: 9841453]
2. Langer R, Vacanti JP. Tissue Engineering. Science. 1993; 260:920–926. [PubMed: 8493529]
3. Blow N. Biobanking: Freezer Burn. Nat Methods. 2009; 6:173–178.
4. Toner M, Kocsis J. Storage and Translational Issues in Reparative Medicine. Ann N Y Acad Sci. 2002; 961:258–262. [PubMed: 12081912]
5. Pancrazio JJ, Wang F, Kelley CA. Enabling Tools for Tissue Engineering. Biosens Bioelectron. 2007; 22:2803–2811. [PubMed: 17240132]
6. Meyers SA. Dry Storage of Sperm: Applications in Primates and Domestic Animals. Reprod, Fertil Dev. 2006; 18:1–5. [PubMed: 16478596]
7. He X. Thermostability of Biological Systems: Fundamentals, Challenges, and Quantification. Open Biomed Eng J. 2011; 5:47–73. [PubMed: 21769301]
8. Ock SA, Rho GJ. Effect of Dimethyl Sulfoxide (Dmso) on Cryopreservation of Porcine Mesenchymal Stem Cells (Pmscs). Cell Transplant. 2011; 20:1231–1239. [PubMed: 21294964]
9. Hunt CJ. Cryopreservation of Human Stem Cells for Clinical Application: A Review. Transfus Med Hemother. 2011; 38:107–123. [PubMed: 21566712]
10. Rosland GV, Svendsen A, Torsvik A, Sobala E, McCormack E, Immervoll H, Mysliwietz J, Tonn JC, Goldbrunner R, Lonning PE, et al. Long-Term Cultures of Bone Marrow-Derived Human Mesenchymal Stem Cells Frequently Undergo Spontaneous Malignant Transformation. Cancer Res. 2009; 69:5331–5339. [PubMed: 19509230]
11. Izadpanah R, Kaushal D, Kriedt C, Tsien F, Patel B, Dufour J, Bunnell BA. Long-Term in Vitro Expansion Alters the Biology of Adult Mesenchymal Stem Cells. Cancer Res. 2008; 68:4229–4238. [PubMed: 18519682]
12. Froelich K, Mickler J, Steusloff G, Technau A, Ramos Tirado M, Scherzed A, Hackenberg S, Radeloff A, Hagen R, Kleinsasser N. Chromosomal Aberrations and Deoxyribonucleic Acid Single-Strand Breaks in Adipose-Derived Stem Cells During Long-Term Expansion in Vitro. Cytotherapy. 2013; 15:767–781. [PubMed: 23643417]
13. Capelli C, Pedrini O, Cassina G, Spinelli O, Salmoiraghi S, Golay J, Rambaldi A, Giussani U, Introna M. Frequent Occurrence of Non-Malignant Genetic Alterations in Clinical Grade Mesenchymal Stromal Cells Expanded for Cell Therapy Protocols. Haematologica. 2014; 99:e94–97. [PubMed: 24682511]
14. Pan Q, Fouraschen SM, de Ruiter PE, Dinjens WN, Kwekkeboom J, Tilanus HW, van der Laan LJ. Detection of Spontaneous Tumorigenic Transformation During Culture Expansion of Human Mesenchymal Stromal Cells. Exp Biol Med. 2014; 239:105–115.
15. Liu H, Lin J, Roy K. Effect of 3d Scaffold and Dynamic Culture Condition on the Global Gene Expression Profile of Mouse Embryonic Stem Cells. Biomaterials. 2006; 27:5978–5989. [PubMed: 16824594]
16. Scadden DT. The Stem-Cell Niche as an Entity of Action. Nature. 2006; 441:1075–1079. [PubMed: 16810242]
17. McDevitt TC, Palecek SP. Innovation in the Culture and Derivation of Pluripotent Human Stem Cells. Curr Opin Biotechnol. 2008; 19:527–533. [PubMed: 18760357]
18. Karlsson JOM, Toner M. Long-Term Storage of Tissues by Cryopreservation: Critical Issues. Biomaterials. 1996; 17:243–256. [PubMed: 8745321]
19. Meryman HT. Cryoprotective Agents. Cryobiology. 1971; 8:173–183. [PubMed: 5578883]
20. Davis JM, Rowley SD, Braine HG, Piantadosi S, Santos GW. Clinical Toxicity of Cryopreserved Bone Marrow Graft Infusion. Blood. 1990; 75:781–786. [PubMed: 2297578]
21. Windrum P, Morris TCM, Drake MB, Niederwieser D, Ruutu T, Par ECLW. Variation in Dimethyl Sulfoxide Use in Stem Cell Transplantation: A Survey of Ebmt Centres. Bone Marrow Transplant. 2005; 36:601–603. [PubMed: 16044141]

22. Chetty S, Pagliuca FW, Honore C, Kweudjeu A, Rezania A, Melton DA. A Simple Tool to Improve Pluripotent Stem Cell Differentiation. Nat Methods. 2013; 10:553–556. [PubMed: 23584186]
23. Crowe JH, Crowe LM. Preservation of Mammalian Cells-Learning Nature's Tricks. Nat Biotechnol. 2000; 18:145–146. [PubMed: 10657114]
24. Crowe JH. Trehalose as a "Chemical Chaperone": Fact and Fantasy. Adv Exp Med Biol. 2007; 594:143–158. [PubMed: 17205682]
25. Rothschild LJ, Mancinelli RL. Life in Extreme Environments. Nature. 2001; 409:1092–1101. [PubMed: 11234023]
26. Crowe J, Crowe L, Carpenter J. Preserving Dry Biomaterials: The Water Replacement Hypothesis Part I. Biopharm. 1993; 6:28–33.
27. Crowe J, Crowe L, Carpenter J. Preserving Dry Biomaterials: The Water Replacement Hypothesis, Part Ii. Biopharm. 1993; 6:40–43.
28. Clegg JS, Seitz P, Seitz W, Hazlewood CF. Cellular Responses to Extreme Water Loss: The Water-Replacement Hypothesis. Cryobiology. 1982; 19:306–316. [PubMed: 7105783]
29. Cottone G. A Comparative Study of Carboxy Myoglobin in Saccharide-Water Systems by Molecular Dynamics Simulation. J Phys Chem B. 2007; 111:3563–3569. [PubMed: 17388507]
30. Cottone G, Giuffrida S, Ciccotti G, Cordone L. Molecular Dynamics Simulation of Sucrose- and Trehalose-Coated Carboxy-Myoglobin. Proteins. 2005; 59:291–302. [PubMed: 15723350]
31. D'Alfonso L, Collini M, Baldini G. Trehalose Influence on Beta-Lactoglobulin Stability and Hydration by Time Resolved Fluorescence. Eur J Biochem. 2003; 270:2497–2504. [PubMed: 12755705]
32. Roche CJ, Guo F, Friedman JM. Molecular Level Probing of Preferential Hydration and Its Modulation by Osmolytes through the Use of Pyranine Complexed to Hemoglobin. J Biol Chem. 2006; 281:38757–38768. [PubMed: 17057250]
33. Crowe JH, Carpenter JF, Crowe LM. The Role of Vitrification in Anhydrobiosis. Annu Rev Physiol. 1998; 60:73–103. [PubMed: 9558455]
34. He XM, Fowler A, Toner M. Water Activity and Mobility in Solutions of Glycerol and Small Molecular Weight Sugars: Implication for Cryo- and Lyopreservation. J Appl Phys. 2006; 100:074702 (074711pp).
35. Crowe JH, Crowe LM, Oliver AE, Tsvetkova N, Wolkers W, Tablin F. The Trehalose Myth Revisited: Introduction to a Symposium on Stabilization of Cells in the Dry State. Cryobiology. 2001; 43:89–105. [PubMed: 11846464]
36. Sun WQ, Leopold AC, Crowe LM, Crowe JH. Stability of Dry Liposomes in Sugar Glasses. Biophys J. 1996; 70:1769–1776. [PubMed: 8785336]
37. Crowe JH, Tablin F, Wolkers WF, Gousset K, Tsvetkova NM, Ricker J. Stabilization of Membranes in Human Platelets Freeze-Dried with Trehalose. Chem Phys Lipids. 2003; 122:41–52. [PubMed: 12598037]
38. Satpathy GR, Torok Z, Bali R, Dwyre DM, Little E, Walker NJ, Tablin F, Crowe JH, Tsvetkova NM. Loading Red Blood Cells with Trehalose: A Step Towards Biostabilization. Cryobiology. 2004; 49:123–136. [PubMed: 15351684]
39. Sun WQ, Davidson P. Protein Inactivation in Amorphous Sucrose and Trehalose Matrices: Effects of Phase Separation and Crystallization. Biochim Biophys Acta. 1998; 1425:235–244. [PubMed: 9813347]
40. Wolkers WF, Tablin F, Crowe JH. From Anhydrobiosis to Freeze-Drying of Eukaryotic Cells. Comp Biochem Physiol, Part A: Mol Integr Physiol. 2002; 131:535–543.
41. Wolkers WF, Walker NJ, Tablin F, Crowe JH. Human Platelets Loaded with Trehalose Survive Freeze-Drying. Cryobiology. 2001; 42:79–87. [PubMed: 11448110]
42. Seetharam RN, Blum AS, Soto CM, Whitley JL, Sapsford KE, Chatterji A, Lin T, Johnson JE, Guerra C, Satir P, et al. Long Term Storage of Virus Templated Fluorescent Materials for Sensing Applications. Nanotechnology. 2008; 19:105504 (105507pp). [PubMed: 21817702]
43. Chen T, Acker JP, Eroglu A, Cheley S, Bayley H, Fowler A, Toner M. Beneficial Effect of Intracellular Trehalose on the Membrane Integrity of Dried Mammalian Cells. Cryobiology. 2001; 43:168–181. [PubMed: 11846471]

44. Eroglu A, Toner M, Toth TL. Beneficial Effect of Microinjected Trehalose on the Cryosurvival of Human Oocytes. Fertil Steril. 2002; 77:152–158. [PubMed: 11779606]
45. Acker, JP.; Chen, T.; Fowler, A.; Toner, M. Life in the Frozen State. Boca Raton, FL: CRC Press LLC; 2004. Engineering Desiccation Tolerance in Mammalian Cells: Tools and Techniques; p. 563-581.
46. Bhowmick P, Eroglu A, Wright DL, Toner M, Toth TL. Osmometric Behavior of Mouse Oocytes in the Presence of Different Intracellular Sugars. Cryobiology. 2002; 45:183–187. [PubMed: 12482383]
47. Eroglu A, Lawitts JA, Toner M, Toth TL. Quantitative Microinjection of Trehalose into Mouse Oocytes and Zygotes, and Its Effect on Development. Cryobiology. 2003; 46:121–134. [PubMed: 12686202]
48. Eroglu A, Elliott G, Wright DL, Toner M, Toth TL. Progressive Elimination of Microinjected Trehalose During Mouse Embryonic Development. Reprod BioMed Online. 2005; 10:503–510. [PubMed: 15901459]
49. Gordon SL, Oppenheimer SR, Mackay AM, Brunnabend J, Puhlev I, Levine F. Recovery of Human Mesenchymal Stem Cells Following Dehydration and Rehydration. Cryobiology. 2001; 43:182–187. [PubMed: 11846472]
50. Guo N, Puhlev I, Brown DR, Mansbridge J, Levine F. Trehalose Expression Confers Desiccation Tolerance on Human Cells. Nat Biotechnol. 2000; 18:168–171. [PubMed: 10657122]
51. Puhlev I, Guo N, Brown DR, Levine F. Desiccation Tolerance in Human Cells. Cryobiology. 2001; 42:207–217. [PubMed: 11578120]
52. Acker JP, Lu XM, Young V, Cheley S, Bayley H, Fowler A, Toner M. Measurement of Trehalose Loading of Mammalian Cells Porated with a Metal-Actuated Switchable Pore. Biotechnol Bioeng. 2003; 82:525–532. [PubMed: 12652476]
53. Eroglu A, Russo MJ, Bieganski R, Fowler A, Cheley S, Bayley H, Toner M. Intracellular Trehalose Improves the Survival of Cryopreserved Mammalian Cells. Nat Biotechnol. 2000; 18:163–167. [PubMed: 10657121]
54. Liu XH, Aksan A, Menze MA, Hand SC, Toner M. Trehalose Loading through the Mitochondrial Permeability Transition Pore Enhances Desiccation Tolerance in Rat Liver Mitochondria. Biochim Biophys Acta. 2005; 1717:21–26. [PubMed: 16242115]
55. Shirakashi R, Köstner CM, Müller KJ, Kürschner M, Zimmermann U, Sukhorukov VL. Intracellular Delivery of Trehalose into Mammalian Cells by Electropermeabilization. J Membr Biol. 2002; 189:45–54. [PubMed: 12202951]
56. Reuss R, Ludwig J, Shirakashi R, Ehrhart F, Zimmermann H, Schneider S, Weber MM, Zimmermann U, Schneider H, Sukhorukov VL. Intracellular Delivery of Carbohydrates into Mammalian Cells through Swelling-Activated Pathways. J Membr Biol. 2004; 200:67–81. [PubMed: 15520905]
57. Oliver AE, Jamil K, Crowe JH, Tablin F. Loading Mscs with Trehalose by Endocytosis. Cell Preserv Technol. 2004; 2:35–49.
58. Wolkers WF, Looper SA, Fontanilla RA, Tsvetkova NM, Tablin F, Crowe JH. Temperature Dependence of Fluid Phase Endocytosis Coincides with Membrane Properties of Pig Platelets. Biochim Biophys Acta. 2003; 1612:154–163. [PubMed: 12787933]
59. He XM, Amin AA, Fowler A, Toner M. Thermally Induced Introduction of Trehalose into Primary Rat Hepatocytes. Cell Preserv Technol. 2006; 4:178–187.
60. Beattie GM, Crowe JH, Lopez AD, Cirulli V, Ricordi C, Hayek A. Trehalose: A Cryoprotectant That Enhances Recovery and Preserves Function of Human Pancreatic Islets after Long-Term Storage. Diabetes. 1997; 46:519–523. [PubMed: 9032112]
61. Holovati JL, Acker JP. Spectrophotometric Measurement of Intraliposomal Trehalose. Cryobiology. 2007; 55:98–107. [PubMed: 17659270]
62. Scott KL, Gyongyossy-Issa MIC, Acker JP. Response of Hemotopoietic Progenitor Cells to Trehalose-Loaded Liposomes (Abstract). Cryobiology. 2006; 53:380.
63. Holovati JL, Gyongyossy-Issa MIC, Acker JP. Effects of Trehalose-Loaded Liposomes on Red Blood Cell Response to Freezing and Post-Thaw Membrane Quality. Cryobiology. 2009; 58:75–83. [PubMed: 19059392]

64. Zhang W, Rong J, Wang Q, He X. The Encapsulation and Intracellular Delivery of Trehalose Using a Thermally Responsive Nanocapsule. Nanotechnology. 2009; 20:275101. [PubMed: 19528681]

65. Kanias T, Acker JP. Mammalian Cell Desiccation: Facing the Challenges. Cell Preserv Technol. 2006; 4:253–276.

66. Zhang W, Gilstrap K, Wu L, KCR, Moss MA, Wang Q, Lu X, He X. Synthesis and Characterization of Thermally Responsive Pluronic F127-Chitosan Nanocapsules for Controlled Release and Intracellular Delivery of Small Molecules. ACS nano. 2010; 4:6747–6759. [PubMed: 21038924]

67. Rao W, Zhang W, Poventud-Fuentes I, Wang Y, Lei Y, Agarwal P, Weekes B, Li C, Lu X, Yu J, et al. Thermally Responsive Nanoparticle-Encapsulated Curcumin and Its Combination with Mild Hyperthermia for Enhanced Cancer Cell Destruction. Acta Biomater. 2014; 10:831–842. [PubMed: 24516867]

68. Weigel A, Schild D, Zeug A. Resolution in the Apotome and the Confocal Laser Scanning Microscope: Comparison. J Biomed Opt. 2009; 14:014022. [PubMed: 19256710]

69. Cain RJ, d'Agua BB, Ridley AJ. Quantification of Transendothelial Migration Using Three-Dimensional Confocal Microscopy. Cell Migration: Developmental Methods and Protocols, Second Edition. 2011; 769:167–190.

70. Zhang W, Zhao S, Rao W, Snyder J, Choi JK, Wang J, Khan IA, Saleh NB, Mohler PJ, Yu J, et al. A Novel Core-Shell Microcapsule for Encapsulation and 3d Culture of Embryonic Stem Cells. J Mater Chem B. 2013; 1:1002–1009.

71. Chen H, Ouyang W, Lawuyi B, Martoni C, Prakash S. Reaction of Chitosan with Genipin and Its Fluorogenic Attributes for Potential Microcapsule Membrane Characterization. J Biomed Mater Res, Part A. 2005; 75:917–927.

72. Muzzarelli RAA. Genipin-Crosslinked Chitosan Hydrogels as Biomedical and Pharmaceutical Aids. Carbohydr Polym. 2009; 77:1–9.

73. Mi FL, Tan YC, Liang HF, Sung HW. In Vivo Biocompatibility and Degradability of a Novel Injectable-Chitosan-Based Implant. Biomaterials. 2002; 23:181–191. [PubMed: 11762837]

74. Li J, Ren N, Qiu J, Mou X, Liu H. Graphene Oxide-Reinforced Biodegradable Genipin-Cross-Linked Chitosan Fluorescent Biocomposite Film and Its Cytocompatibility. Int J Nanomed. 2013; 8:3415–3426.

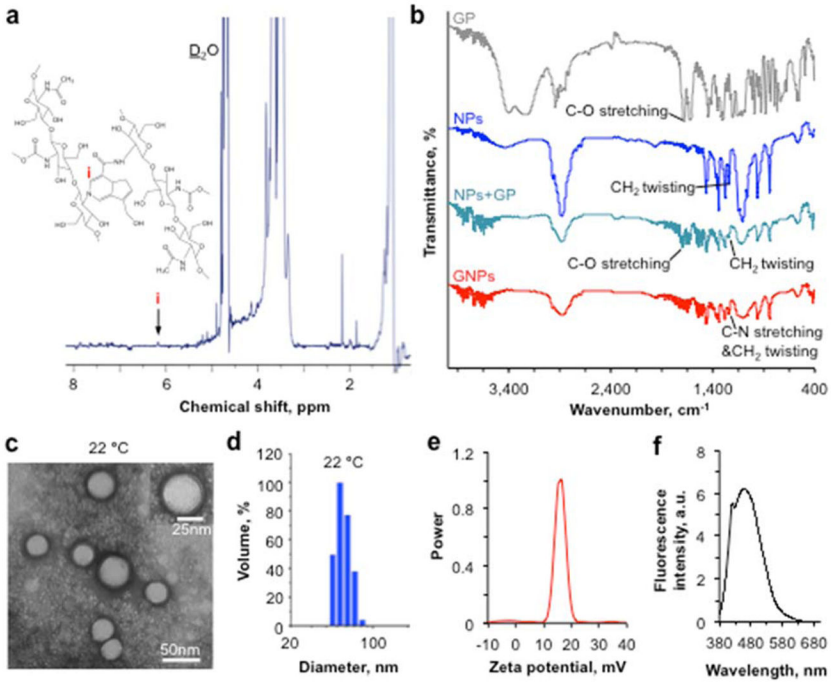

Figure 1.

Characterization of empty genipin-crosslinked Pluronic F127-chitosan nanoparticles (GNPs) showing successful crosslinking between genipin and chitosan in the GNPs and their round shape, nanoscale size, positively charged surface, and blue fluorescent property. a) ^{1}H NMR spectra of GNPs showing a characteristic peak of genipin in the nanomaterial. b) FTIR spectra of genipin (GP), Pluronic F127-chitosan nanoparticles (NPs), a simple mixture of Pluronic F127-chitosan NPs and GP (NPs+GP), and GNPs showing changes in characteristic peaks as a result of the crosslinking reaction between genipin and chitosan. c) A typical TEM image of GNPs showing their round core-shell morphology and nanoscale size at 22 °C (room temperature). d) Typical dynamic light scattering (DLS) data on the size of GNPs dissolved in deionized water at 22 °C. e) DLS data showing zeta potential of the GNPs. f) Fluorescence emission spectrum of the GNPs under excitation of 369 nm laser showing an emission peak at 461 nm.

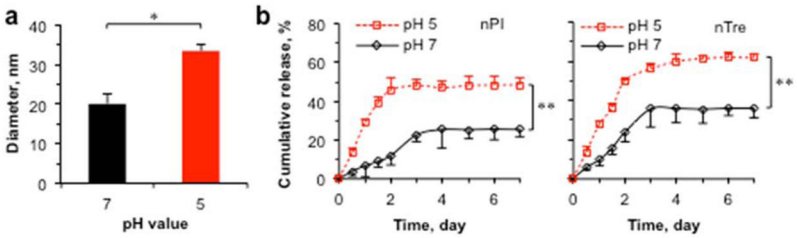

Figure 2.

The pH responsiveness in size and pH-dependent release of nanoparticle-encapsulated PI (nPI) and trehalose (nTre) at 37 °C. a) Size of nTre at pH 7 and 5. b) Cumulative release of PI and trehalose out of the encapsulating GNPs at pH 5 and 7. The nPI and nTre were obtained at 1:10 feeding ratio. *: $p < 0.05$; **: $p < 0.01$

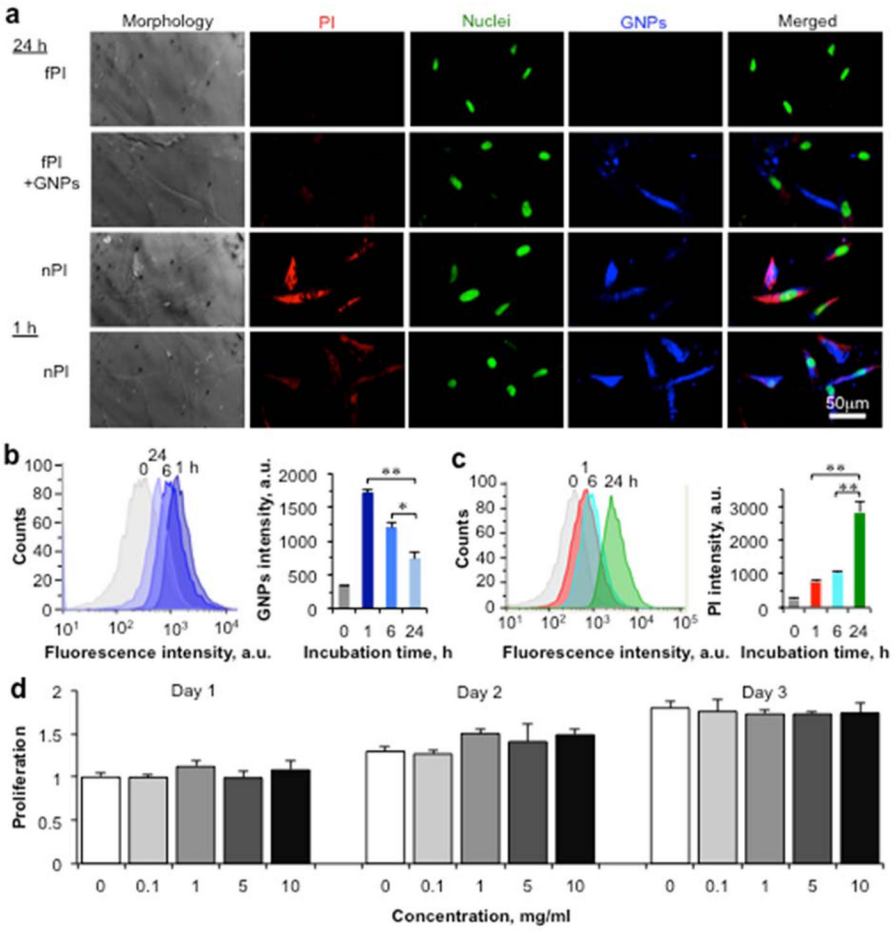

Figure 3.

Cell uptake of nanoparticle-encapsulated PI (nPI) and negligible cytotoxicity of empty GNPs. a) Typical micrographs of primary human adipose-derived stem cells (hADSCs) at 24 h after incubating with free PI, a simple mixture of free PI and GNPs, and nPI together with that after 1 h incubation with nPI. The PI concentration was 0.08 mM for all the conditions. b) Typical flow cytometry peaks and quantitative fluorescence intensity of GNPs in hADSCs incubated with nPI for various times showing quick cell uptake of the GNPs in 1 h and decrease in fluorescence intensity of the GNPs thereafter possibly due to degradation of the GNPs inside the cells. c) Typical flow cytometry peaks and quantitative intensity of PI in the hADSCs incubated with nPI for various times at 37 °C showing significantly higher intracellular PI intensity at 24 h than 1 or 6 h. d) Proliferation of the hADSCs after incubating with empty GNPs at various concentrations for 1, 2 and 3 days. *: $p < 0.05$; **: $p < 0.01$.

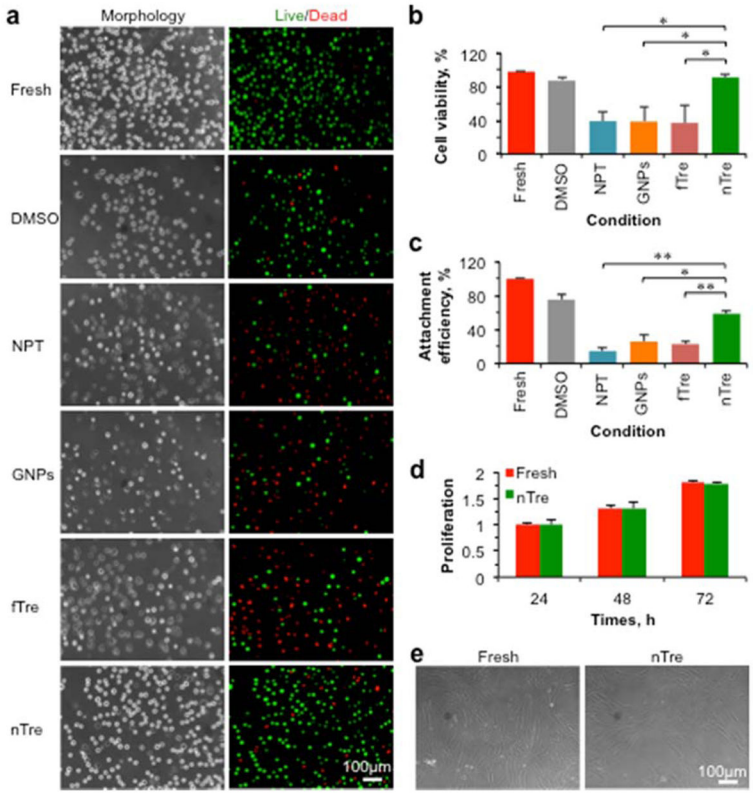

Figure 4.

Intracellular delivery of trehalose with GNPs enables successful cryopreservation of hADSCs using trehalose as the sole cryoprotectant. a) Typical phase and fluorescence micrographs showing high immediate viability of hADSCs after cryopreservation with nanoparticle-encapsulated trehalose (nTre). b) Quantitative data showing similar high immediate cell viability after cryopreservation with nTre to that of hADSCs cryopreserved with dimethyl sulfoxide (DMSO). c) Attachment efficiency calculated as the percentage of the number of attached live cells after one-day culture post cryopreservation out of the number of fresh cells seeded and cultured in the same way. d) Quantitative data showing similar proliferation of cryopreserved (with nTre) to fresh hADSCs. e) Typical phase micrographs showing similar morphology of fresh to cryopreserved (with nTre) hADSCs. Fresh: without any pre-incubation or cryopreservation; NPT: no pre-incubation with trehalose or GNCs for cryopreservation; GNPs: pre-incubated with GNCs for cryopreservation; fTre: pre-incubated with free trehalose for cryopreservation; and nTre: pre-incubated with nTre for cryopreservation. *: $p < 0.05$; **: $p < 0.01$.

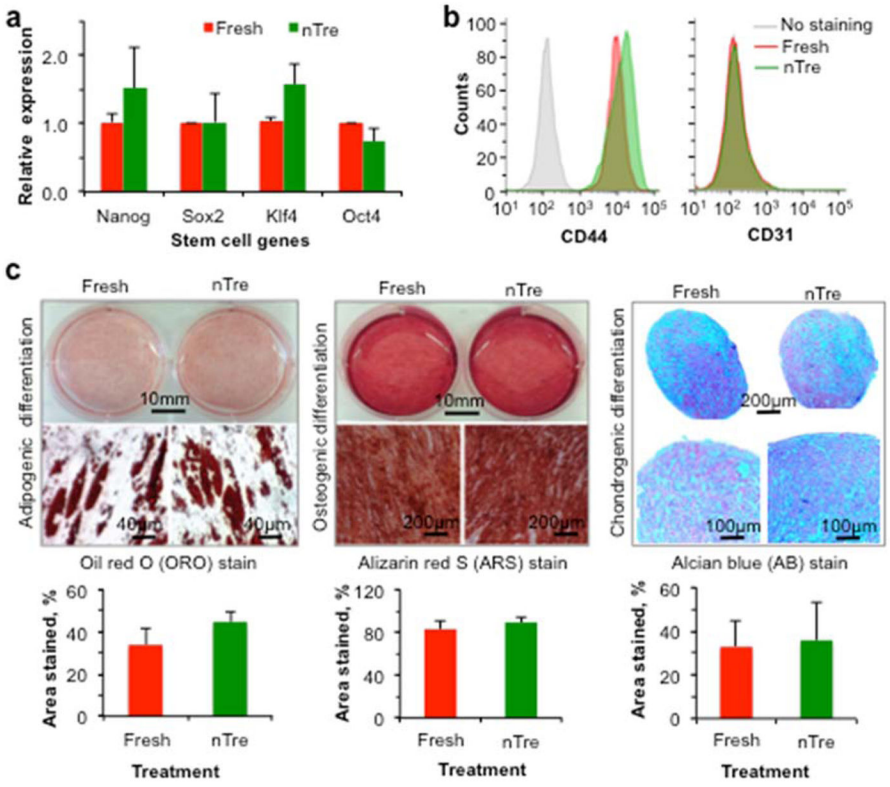

Figure 5.

The hADSCs cryopreserved with nTre retain intact stemness and capability of multi-lineage differentiation. a) Comparable expression of four stem cell genes in fresh and cryopreserved (with nTre) hADSCs. b) Comparable expression of CD44(+) and CD31(−) on fresh and cryopreserved (with nTre) hADSCs. c) Comparable capability of adipogenic, osteogenic, and chondrogenic differentiation of fresh and cryopreserved (with nTre) hADSCs indicated by Oil red O (ORO) stain of lipid-filled droplets, Alizarin red S (ARS) stain of calcific depositions, and Alcian blue (AB) stain of sulfated proteoglycan, respectively.

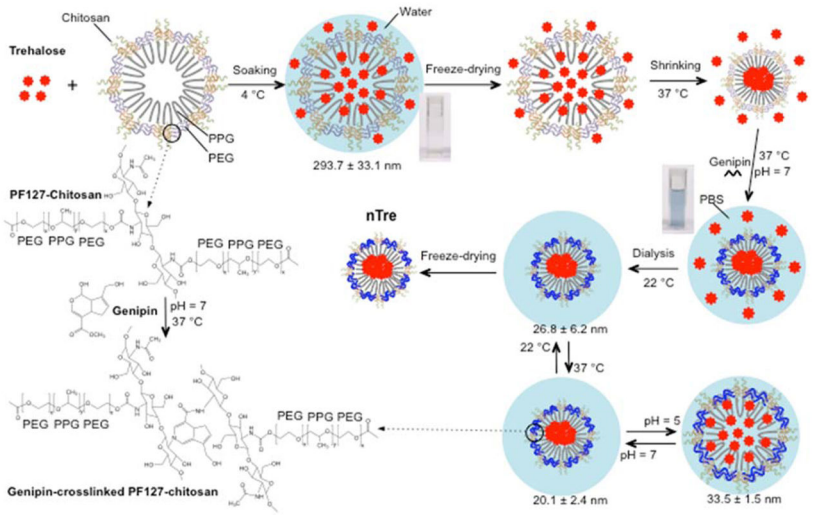

Scheme 1.

A schematic illustration of the procedure for encapsulating hydrophilic (i.e., water-soluble) trehalose in genipin-crosslinked Pluronic F127-chitosan nanoparticles (GNPs) to obtain the nanoparticle-encapsulated trehalose (nTre). After genipin crosslinking, the solution turns from light brown for the aqueous solution of Pluronic F127-chitosan nanoparticles (NPs) into blue for the aqueous solution of GNPs. The GNPs are pH responsive in size at 37 °C although they are not as thermally responsive in size at pH 7 as the Pluronic F127-chitosan NPs. The size (diameter) shown at various temperatures and pH values is for nTre made with a feeding ratio of 1:10 (trehalose:Pluronic F127-chitosan NPs) in weight. PPG: poly(propylene glycol); PEG: poly(ethylene glycol); and PBS: phosphate buffered saline (1x by default)